

Discovery of the Zeeman Effect in the 36 and 44 GHz Class I Methanol Maser Lines with the EVLA

Anuj. P. Sarma

DePaul University

E-mail: asarma@depaul.edu

Emmanuel Momjian*

National Radio Astronomy Observatory

E-mail: emomjian@nrao.edu

We report the discovery of the Zeeman effect in the 36 GHz and the 44 GHz Class I methanol maser lines. The observations were carried out with the Expanded Very Large Array (EVLA) toward the star-forming regions M8E (at 36 GHz) and OMC-2 (at 44 GHz). The detected line of sight magnetic field values are -31.3 ± 3.5 mG and 20.2 ± 3.5 mG to the northwest and southeast of the maser line peak in M8E, respectively, and 18.4 ± 1.1 mG toward the peak of the maser line in OMC-2. The detected fields are comparable and are not significantly different from those measured in the 6.7 GHz Class II methanol maser line toward other star forming regions. This indicates that methanol masers may trace the large scale magnetic field, or that the magnetic field remains unchanged during the early evolution of star forming regions.

ISKAF2010 Science Meeting - ISKAF2010

June 10-14, 2010

Assen, the Netherlands

*Speaker.

1. Introduction

Magnetic fields likely play an important role in the star formation process (e.g., [1], and references therein). The nature of this role is not yet clear, however, primarily due to the scarcity of observational data on magnetic fields in star forming regions. The Zeeman effect remains the most direct method for measuring magnetic field strengths (e.g., [2]). Observations of the Zeeman effect in H I and OH thermal lines have revealed the strength of the magnetic field in the lower density envelopes of molecular clouds (e.g., [3]). Observations of the Zeeman effect in H₂O masers, on the other hand, offer a window into magnetic fields in the highest density regions ($n \sim 10^9 \text{ cm}^{-3}$) of star forming regions [4, 5].

Interstellar masers, being compact and intense, are extremely effective probes of young star forming regions. Recently, Vlemmings (2008) [6] carried out the first systematic study of the Zeeman effect in the 6.7 GHz methanol maser line. Such (6.7 GHz) masers are examples of Class II methanol masers, which are known to be probes of the early phases of high mass star forming regions. Yet another class of masers, namely Class I methanol masers, may probe even earlier phases of star forming regions [7]. This appears to be the case for the star forming regions M8E and OMC-2.

2. Observations and Data Reduction

Observations of the $4_{-1} - 3_0$ methanol maser emission line at 36 GHz in M8E were carried out using the Expanded Very Large Array (EVLA) of the NRAO¹ in two 2 hr sessions on 2009 July 9 and 25. Thirteen EVLA antennas equipped with the 27–40 GHz (Ka-band) receivers were used in these observations. The observations of the $7_0 - 6_1A^+$ methanol maser emission line at 44 GHz in OMC-2 were carried out using 22 EVLA antennas in two 2 hr sessions on October 25 and November 25, 2009. Various observational parameters are listed in Table 1.

The sources 3C286 (J1331+3030) and 3C147 (J0542+4951) were used to set the absolute flux density scales, while the compact sources J1733–1304 and J0607–0834 were used as amplitude calibrators in the 36 and 44 GHz observations, respectively.

The editing, calibration, Fourier transformation, deconvolution, and processing of the data were carried out using the Astronomical Image Processing System (AIPS) of the NRAO. After applying the amplitude gain corrections using the respective calibrator sources in each observation, the spectral channel with the strongest maser emission signal in each source was split, then self-calibrated in both phase and amplitude in a succession of iterative cycles. The final phase and amplitude solutions were then applied on the full spectral-line uv data set, and Stokes I and V image cubes were made, and used for the magnetic field measurements.

3. Analysis

For cases in which the Zeeman splitting $\Delta\nu_z$ is much less than the line width $\Delta\nu$, the magnetic field can be obtained from the Stokes V spectrum, which exhibits a *scaled derivative* of the Stokes I

¹The National Radio Astronomy Observatory (NRAO) is a facility of the National Science Foundation operated under cooperative agreement by Associated Universities, Inc.

spectrum [8]. Here, consistent with AIPS conventions, $I = (\text{RCP} + \text{LCP})/2$, and $V = (\text{RCP} - \text{LCP})/2$; RCP is right- and LCP is left-circular polarization incident on the antennas, where RCP has the standard radio definition of clockwise rotation of the electric vector when viewed along the direction of wave propagation. Since the observed V spectrum may also contain a scaled replica of the I spectrum itself, the Zeeman effect can be measured by fitting the Stokes V spectra in the least-squares sense to the equation

$$V = aI + \frac{b}{2} \frac{dI}{dv} \quad (3.1)$$

[9, 10]. The fit parameter a is usually the result of small calibration errors in RCP versus LCP, and is expected to be small. In these observations, a was of the order of 10^{-4} or less. While eq. 3.1 is strictly true only for thermal lines, numerical solutions of the equations of radiative transfer (e.g., [11]) have shown that it gives reasonable values for the magnetic fields in masers also. In eq. 3.1, the fit parameter $b = zB \cos \theta$, where z is the Zeeman splitting factor (Hz mG^{-1}), B is the magnetic field, and θ is the angle of the magnetic field to the line of sight [12]. Following the treatment of Vlemmings (2008) for the Zeeman splitting of 6.7 GHz methanol masers, we derive the Zeeman splitting factor using the Landé g -factor based on laboratory measurements of 25 GHz methanol masers [13], and find $z = 1.7 \text{ Hz mG}^{-1}$ for 36 GHz, and $z = 1.0 \text{ Hz mG}^{-1}$ for 44 GHz methanol masers. While this will likely introduce a systematic bias into the magnetic field results, it remains the best possible estimate pending laboratory measurements of the 36 and 44 GHz maser lines.

4. Results & Discussion

To demonstrate our detection of the Zeeman effect in the 36 GHz Class I methanol maser line toward M8E, we display the Stokes I and V profiles toward two positions in this source in Fig. 1; the two positions are to the northwest and southeast of the maser line peak. In Fig. 2, we show the Stokes I and V profiles toward the peak emission region of the 44 GHz Class I methanol maser line toward OMC-2.

As described in the previous section, we determined magnetic fields by fitting the Stokes V spectra in the least-squares sense using equation 3.1. Using the Zeeman splitting factor $z = 1.7 \text{ Hz mG}^{-1}$ we derived $B_{\text{los}} = -31.3 \pm 3.5 \text{ mG}$ for the northwest position of M8E, and $20.2 \pm 3.5 \text{ mG}$ for its southeast position. By convention, a negative value for B_{los} indicates a field pointing toward the observer. Meanwhile, in OMC-2, we used $z = 1.0 \text{ Hz mG}^{-1}$ and derived $B_{\text{los}} = 18.4 \pm 1.1 \text{ mG}$.

In M8E, the line-of-sight magnetic field has opposite signs at the two positions for which Stokes I and V profiles are shown in Fig. 1, with values of -31.3 mG and 20.2 mG , respectively. The observed change in the sign of B_{los} at these two positions, together with a slight asymmetry in the maser line profiles at each position, indicates that we are observing at least two masers that are very close in position and velocity. The masers are marginally resolved in our C-configuration observations, otherwise the opposite magnetic fields would sum to zero. EVLA B- or A-configuration observations will be necessary to fully resolve the maser components. The observed change in sign of B_{los} occurs over a size scale of $0.9''$, equal to 1300 AU (assuming the distance to M8E is 1.5 kpc). This may mean that the clumps where the 36 GHz maser is being excited come from two different regions where the field is truly different. Alternatively, it may mean that the field lines curve across the region in which the masers are being excited, so that the line-of-sight field traced by one maser

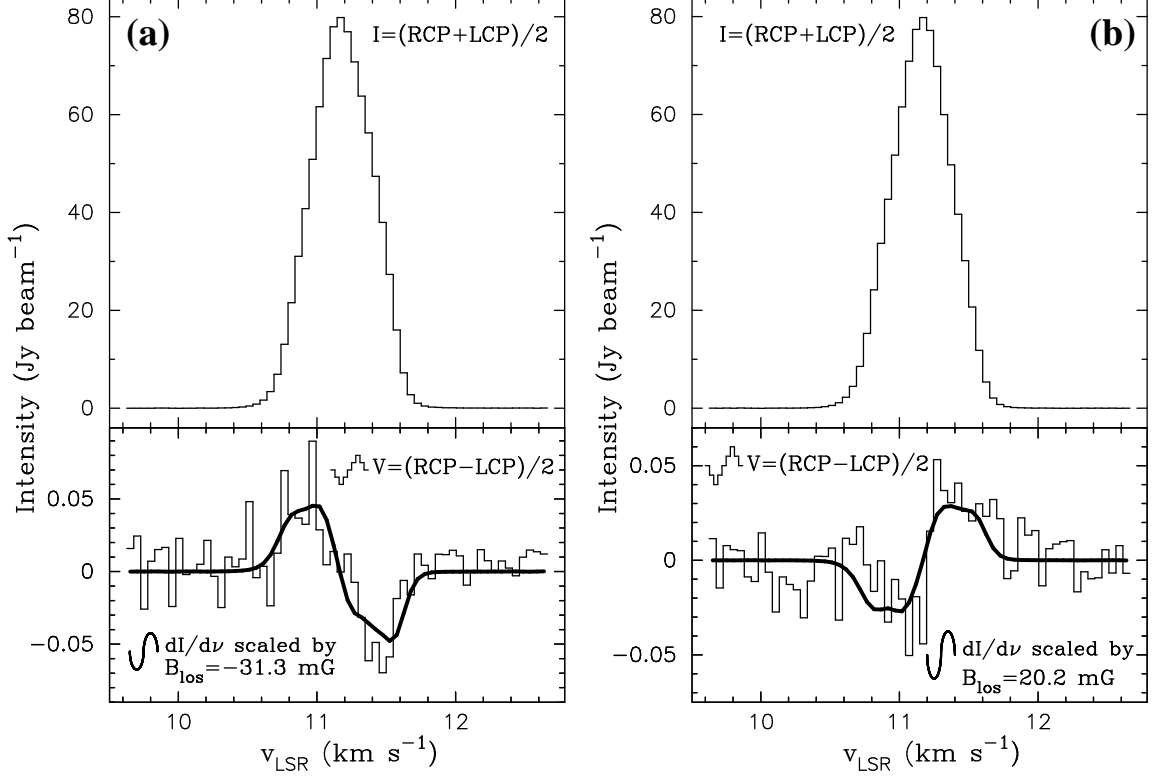


Figure 1: Stokes I (top-histogram) and V (bottom-histogram) profiles of the maser toward the (a) northwest and (b) southeast of the 36 GHz Class I methanol maser line peak in M8E. The curve superposed on V in each of the lower frames is the derivative of I scaled by a value of $B_{\text{los}} = -31.3 \pm 3.5$ mG in (a), and $B_{\text{los}} = 20.2 \pm 3.5$ mG in (b).

is pointed toward us, whereas that traced by the other maser is pointed away from us. For more details on the discovery of the Zeeman effect in the 36 GHz Class I methanol maser line toward M8E, we refer to the article by Sarma & Momjian (2009) [14].

Our detected B_{los} values in the 36 GHz and 44 GHz Class I methanol maser lines toward M8E and OMC-2 are similar to the values obtained in the 6.7 GHz Class II methanol maser line toward other sources [6]. Vlemmings (2008) detected significant magnetic fields in 6.7 GHz methanol masers with the 100 m Effelsberg telescope in 17 sources, with an average value of 23 mG. Since Class I and Class II methanol masers trace different spatial regions, this may indicate that the magnetic field is the same over the extent of these two regions, giving rise to the possibility that methanol masers trace the large-scale magnetic field in the star forming region. Alternatively, if Class I masers occur in the very early stages of star formation (before the formation of an ultra-compact H II region), and Class II masers occur later on, the similarity in B_{los} for these two classes, if true, may indicate that the magnetic field strength remains the same during the early stages of the star formation process. Certainly, more observations are necessary, especially in regions where both Class I and Class II masers are known to occur, in order to address the possibilities noted above.

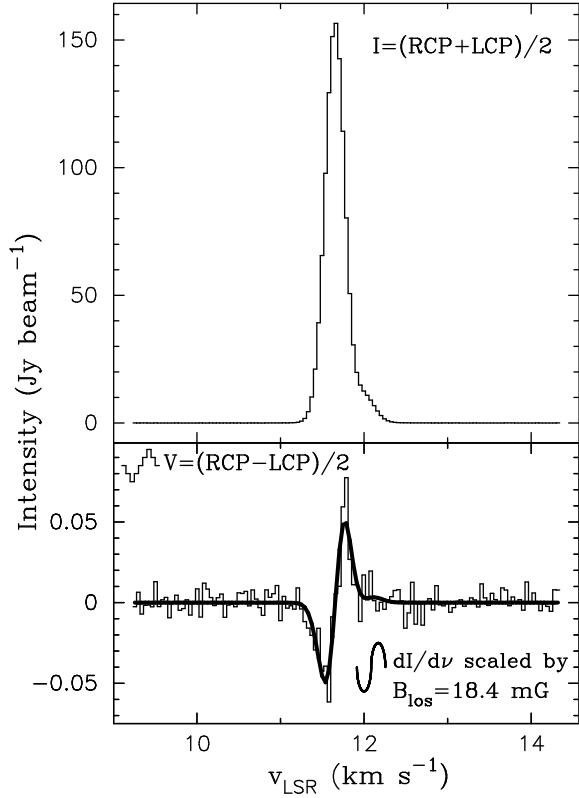


Figure 2: Stokes I (top-histogram) and V (bottom-histogram) profiles of the maser toward the peak of the 44 GHz Class I methanol maser line in OMC-2. The curve superposed on V in each of the lower frames is the derivative of I scaled by a value of $B_{\text{los}} = 18.4 \pm 1.1$ mG.

Parameter	M8E	OMC-2
Observation Dates	2009 July 9 & 25	2009 October 25 & November 25
Configuration	C	D
R.A. of field center (J2000)	18:04:53.3	05:35:27.66
Decl. of field center (J2000)	-24:26:42.0	-05:09:39.6
Total Bandwidth	1.56 MHz	1.56 MHz
No. of channels	256	256
Channel Spacing	0.05 km s ⁻¹	0.04 km s ⁻¹
Total Observing Time	4 hr	4 hr
Rest Frequency	36.16929 GHz	44.069488 GHz
Target source velocity	11.2 km s ⁻¹	11.6 km s ⁻¹

Table 1: Parameters of the EVLA Observations

References

- [1] Troland, T. H., Heiles, C., Sarma, A. P., Ferland, G. J., Crutcher, R. M., & Brogan, C. L. 2008, arXiv:0804.3396.
- [2] Crutcher, R. M. 1999, ApJ, 520, 706.
- [3] Brogan, C. L., & Troland, T. H. 2001, ApJ, 560, 821.
- [4] Sarma, A. P., Troland, T. H., Romney, J. D., & Huynh, T. H. 2008, ApJ, 674, 295.
- [5] Vlemmings, W. H. T., Diamond, P. J., van Langevelde, H. J., & Torrelles, J. M. 2006, A&A, 448, 597.
- [6] Vlemmings, W. H. T. 2008, A&A, 484, 773.
- [7] Pratap, P., Shute, P. A., Keane, T. C., Battersby, C., & Sterling, S. 2008, AJ, 135, 1718.
- [8] Heiles, C., Goodman, A. A., McKee, C. F., & Zweibel, E. G. 1993, in *Protostars and Planets III*, ed. E. H. Levy & J. I. Lunine (Tucson: Univ. Arizona Press), 279.
- [9] Troland, T. H., & Heiles, C. 1982, ApJ, 252, 179.
- [10] Sault, R. J., Killeen, N. E. B., Zmuidzinas, J., & Loushin, R. 1990, ApJS, 74, 437.
- [11] Nedoluha, G. E., & Watson, W. D. 1992, ApJ, 384, 185.
- [12] Crutcher, R. M., Troland, T. H., Goodman, A. A., Heiles, C., Kazes, I., & Myers, P. C. 1993, ApJ, 407, 175.
- [13] Jen, C. K. 1951, Physical Review, 81, 197.
- [14] Sarma, A. P., & Momjian, E., 2009, ApJ, 705, L176.